

Fundamental limits of quantum illumination

Ranjith Nair^{1,2,*} and Mile Gu^{1,2,3}

¹ School of Physical and Mathematical Sciences,
Nanyang Technological University, 639673, Singapore

² Complexity Institute, Nanyang Technological University, 639673, Singapore and
³ Centre for Quantum Technologies, 117543, Singapore

(Dated: May 30, 2022)

In Quantum Illumination (QI), a signal beam initially entangled with an idler beam held at the receiver interrogates a target region bathed in thermal background light, and the returned beam is jointly measured with the idler in order to determine whether a weakly reflecting target is present. Using tools from quantum information theory, we derive lower bounds on the error probability of detecting both specular and fading targets and on the mean squared error of estimating the reflectance of a detected target, which are obeyed by any QI transmitter satisfying a signal energy constraint. For bright thermal backgrounds, we show that the QI system using multiple copies of low-brightness two-mode squeezed vacuum states is nearly optimal. More generally, our results provide benchmarks for the best possible performance that can be expected from QI systems at all wavelengths, and at all signal and background noise levels.

Quantum illumination (QI) is a quantum sensing protocol (see [1] for an overview of photonic quantum sensing) introduced by Lloyd [2] in which entanglement shared between a signal beam interrogating a target region and a locally held idler beam can be used to detect the presence of a weakly reflecting target better than any strategy using only a signal beam of the same energy, i.e., average photon number. In particular, Tan et al. showed that using multiple signal-idler modes prepared in the two-mode squeezed vacuum (TMSV) state allows a 6 dB improvement of the error probability exponent relative to a classical ladar (laser detection and ranging) system using the same energy [3]. Surprisingly – and unlike other sensing applications for which quantum advantage quickly disappears in the presence of decoherence [4, 5] – this QI advantage obtains when the target is bathed in background thermal radiation of brightness (i.e., per-mode energy) $N_B \gg 1$, due to which the initial signal-idler entanglement is lost. These results inspired much theoretical [6–14] and experimental [15–18] work in QI, most of which is reviewed in the recent article [19]. Beyond the continuous-variable bosonic setting, the original proposal [2] has also been adapted to the discrete-variable setting [20–22].

In this paper, we use tools from quantum information [23] to investigate the fundamental limits of bosonic QI systems in all regimes of signal and background noise strength and allowing for all possible choices of quantum states at the transmitter and quantum measurements at the receiver. We first derive a lower bound on the average error probability of any QI system that transmits an M -mode signal beam entangled with locally held idler modes under a total signal energy constraint \mathcal{N}_S . For $N_B \gg 1$, we show that the scheme of [3] using independently and identically distributed (iid) copies of TMSV states with signal brightness $N_S \equiv \mathcal{N}_S/M \ll 1$ achieves the greatest

error probability exponent allowed by quantum mechanics, and that its near optimality persists for the detection of targets exhibiting flat Rayleigh fading. We also show that any QI system for estimating the reflectance of a detected target has a mean squared error that is at least half that suffered by the best classical ladar.

I. QI SETUP AND BACKGROUND

A general QI setup is depicted schematically in Fig. 1. A transmitter prepares a quantum state of M entangled signal (denoted S) modes (annihilation operators $\{\hat{a}_S^{(m)}\}_{m=1}^M$) and idler (denoted I) modes (annihilation operators $\{\hat{a}_I^{(m)}\}_{m=1}^M$). The signal modes interrogate a target region which may contain a weakly reflecting target of reflectance $\eta \ll 1$ bathed in background (denoted B) noise (annihilation operators $\{\hat{a}_B^{(m)}\}_{m=1}^M$). The annihilation operators $\{\hat{a}_R^{(m)}\}_{m=1}^M$ of the modes returned from the target region, which may acquire an additional phase shift ϕ , obey the relation

$$\hat{a}_R^{(m)} = \sqrt{\eta_h} e^{i\phi} \hat{a}_S^{(m)} + \sqrt{1 - \eta_h} \hat{a}_B^{(m)}. \quad (1)$$

Here $h = 0$ (1) indicates the absence (presence) of a target, $\eta_0 = 0$, and $\eta_1 = \eta$. The two hypotheses are assigned prior probabilities $\{\pi_h\}_{h=0}^1$. In order to focus on the fundamental physical limits, we assume initially that the target is specular and that the values of η and ϕ are known to the receiver. As in previous works [6–14], each background mode is assumed to be in a thermal state $\rho_{\text{th}}(N_B^{(h)}) = \sum_{n=0}^{\infty} N_B^{(h)n} / (N_B^{(h)} + 1)^{n+1} |n\rangle \langle n|_B$ ($\{|n\rangle_B\}$ are number states of B) of brightness

$$\left\langle \hat{a}_B^{(m)\dagger} \hat{a}_B^{(m)} \right\rangle_h \equiv N_B^{(h)} = N_B / (1 - \eta_h) \quad (2)$$

under hypothesis h , where N_B is a given nominal value of the background brightness. (2) ensures that the two

* nairanjith@gmail.com

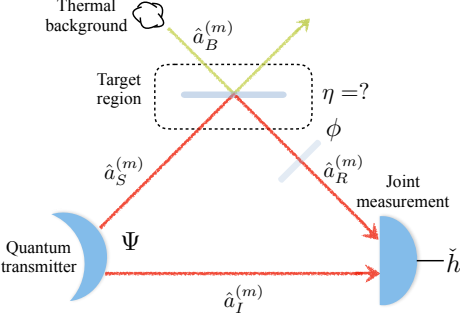


FIG. 1. General setup for QI: A state Ψ entangled between M signal modes and idler modes is prepared. Each signal mode $\hat{a}_S^{(m)}$ interrogates a distant target region bathed in thermal radiation $\hat{a}_B^{(m)}$ which may contain a target of reflectance $\eta \ll 1$. The modes $\{\hat{a}_R^{(m)}\}_{m=1}^M$ returned from the target region are measured jointly with the unperturbed idler modes $\{\hat{a}_I^{(m)}\}_{m=1}^M$ in order to decide whether or not the target was present.

hypotheses are indistinguishable if a vacuum state is transmitted. Since $\eta \ll 1$ for standoff sensing, we have $N_B^{(1)} \simeq N_B$.

Let $|\mathbf{n}\rangle_S$ denote a product number state of the M signal modes with $\mathbf{n} = (n_1, \dots, n_M)$. The most general QI strategy consists of preparing a pure quantum state

$$|\psi\rangle_{IS} = \sum_{\mathbf{n}} \sqrt{p_{\mathbf{n}}} |\chi_{\mathbf{n}}\rangle_I |\mathbf{n}\rangle_S, \quad (3)$$

of the IS system (called *transmitter* hereafter) subject only to the total signal energy constraint

$$\sum_{\mathbf{n}} p_{\mathbf{n}} (n_1 + \dots + n_M) \equiv \sum_{n=0}^{\infty} n p_n = \mathcal{N}_S. \quad (4)$$

Here, $\{|\chi_{\mathbf{n}}\rangle_I\}$ is any normalized set of idler states and $\{p_n\}$ is the probability mass function of the *total* photon number $n = \sum_{m=1}^M n_m$ in the S modes. In the Schrödinger picture, the evolution (1) corresponds to the output density operators

$$\rho_h = \left[\text{id}_I \otimes \left(\mathcal{U}_\phi \circ \mathcal{L}_{\eta_h, N_B^{(h)}} \right)^{\otimes M} \right] (\Psi), \quad (5)$$

where $\Psi = |\psi\rangle \langle \psi|_{IS}$, id_I denotes the identity channel on I , and the unitary phase-shift channel \mathcal{U}_ϕ and the *noisy attenuator channel* of transmittance η_h and added noise $N_B^{(h)}$ (see Fig. 2, [24]) $\mathcal{L}_{\eta_h, N_B^{(h)}}$ act on each mode of S . Note that $\rho_0 = (\text{Tr}_S \Psi) \otimes \rho_{\text{th}}(N_B)$ regardless of the value of ϕ .

The receiver makes the joint measurement on the returned and idler modes with outcome $\check{h} \in \{0, 1\}$ that minimizes the average error probability

$$P_e [\rho_0, \rho_1] = \pi_0 P_F + \pi_1 P_M, \quad (6)$$

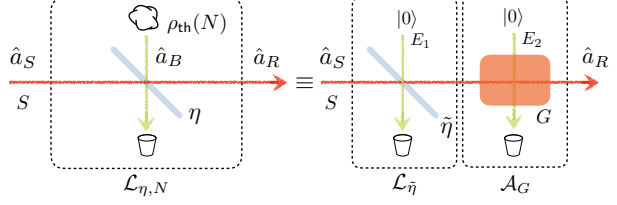


FIG. 2. (Left): A noisy attenuator channel $\mathcal{L}_{\eta, N}$ mixes the signal mode S with a background mode B in a thermal state of energy N at a beamsplitter of transmittance η . (Right): $\mathcal{L}_{\eta, N}$ can be realized as a cascade of a quantum-limited (environment modes E_1 and E_2 in vacuum) loss channel $\mathcal{L}_{\tilde{\eta}}$ of transmittance $\tilde{\eta} = \eta/G$ and optical parametric amplifier (OPA) \mathcal{A}_G of gain $G = (1 - \eta)N + 1$.

where $P_F = \Pr[\check{h} = 1 | h = 0]$ is the false-alarm probability and $P_M = \Pr[\check{h} = 0 | h = 1]$ is the miss probability. The lowest achievable P_e is given by the *Helstrom limit* [25]:

$$P_e [\rho_0, \rho_1] = 1/2 - \|\pi_0 \rho_0 - \pi_1 \rho_1\|_1 / 2, \quad (7)$$

where $\|X\|_1 = \text{Tr} \sqrt{X^\dagger X}$ is the operator trace norm. Since the trace norm is hard to calculate, we often resort to bounds on it.

To be useful, a QI system must have a lower P_e than the best classical radar, i.e., a transmitter that is in a coherent state or mixture of coherent states possibly classically correlated with idler modes. In [3], it was shown that no classical radar with signal energy \mathcal{N}_S can have an error probability lower than

$$P_e^{\text{cl}} \simeq \sqrt{\pi_0 \pi_1} \exp \left[-\eta \mathcal{N}_S \left(\sqrt{N_B + 1} - \sqrt{N_B} \right)^2 \right]. \quad (8)$$

In particular, the exponent after the minus sign in the above expression is the best possible for a classical radar and $\simeq \eta \mathcal{N}_S / 4N_B$ in the regime $N_B \gg 1$. In [3], it was also shown that the transmitter consisting of M copies of the TMSV state $|\psi\rangle_{I_m S_m} = \sum_{n=0}^{\infty} \sqrt{N_S^n / (N_S + 1)^{n+1}} |n\rangle_{I_m} |n\rangle_{S_m}$ has error probability

$$P_e^{\text{TMSV}} \simeq \sqrt{\pi_0 \pi_1} \exp(-\eta \mathcal{N}_S / N_B) \quad (9)$$

in the regime of signal brightness $N_S = \mathcal{N}_S / M \ll 1$ and noise brightness $N_B \gg 1$, which is a 6 dB error exponent advantage over the classical bound (8) at the same \mathcal{N}_S .

II. METHODS AND RESULTS

In this paper, we are interested in performance bounds valid for arbitrary transmitters Ψ . A key tool we use is the decomposition of the noisy attenuator channels appearing in (5) in terms of quantum-limited attenuators

and amplifiers. Specifically, we can write $\mathcal{L}_{\eta,N}$ as the concatenation (see Fig. 2)

$$\mathcal{L}_{\eta,N} = \mathcal{A}_G \circ \mathcal{L}_{\tilde{\eta}}, \quad (10)$$

with $G = (1 - \eta)N + 1$ and $\tilde{\eta} = \eta/G$ [26, 27]. Here $\mathcal{L}_{\tilde{\eta}} := \mathcal{L}_{\tilde{\eta},0}$.

We also make much use of the *fidelity* between two states ρ and σ of a quantum system defined as $F(\rho, \sigma) = \text{Tr} \sqrt{\sqrt{\rho} \sigma \sqrt{\rho}}$, which is an important measure of closeness between quantum states [23]. The fidelity satisfies the *data processing inequality* $F(\mathcal{C}(\rho), \mathcal{C}(\sigma)) \geq F(\rho, \sigma)$, where \mathcal{C} is any quantum channel [23].

A. Lower bound on QI error probability

We begin by using Eqs. (2) and (10) to write

$$\mathcal{L}_{\eta_h, N_B^{(h)}} = \mathcal{A}_{N_B+1} \circ \mathcal{L}_{\eta_h/(N_B+1)} \equiv \mathcal{A}_{N_B+1} \circ \mathcal{L}_{\tilde{\eta}_h}. \quad (11)$$

Then, for any Ψ , we use the data processing inequality to get

$$F(\rho_0, \rho_1) \geq F\left(\left[\text{id}_I \otimes \mathcal{L}_{\tilde{\eta}_0}^{\otimes M}\right](\Psi), \left[\text{id}_I \otimes \mathcal{L}_{\tilde{\eta}_1}^{\otimes M}\right](\Psi)\right) \quad (12)$$

$$\geq \sum_n p_n \mu^n, \quad (13)$$

where $\mu = \sqrt{1 - \eta/(N_B + 1)}$, and the last inequality follows from the result of [28], Sec. II. Using the inequalities $P_e[\sigma_0, \sigma_1] \geq \left(1 - \sqrt{1 - 4\pi_0\pi_1 F^2(\sigma_0, \sigma_1)}\right)/2 \geq \pi_0\pi_1 F^2(\sigma_0, \sigma_1)$ relating the Helstrom limit (7) and the fidelity for any two states σ_0 and σ_1 [29], we get the bound

$$P_e^\Psi \geq \pi_0\pi_1 \left\{ \sum_{n=0}^{\infty} p_n \left[1 - \eta/(N_B + 1)\right]^{n/2} \right\}^2 \quad (14)$$

on the P_e of any Ψ . Further, convexity of the function $x \mapsto \mu^x$ and Jensen's inequality give the Ψ -independent bound

$$P_e^{\text{QI}} \geq \pi_0\pi_1 \exp(-\beta\mathcal{N}_S), \quad (15)$$

where we have defined the exponent $\beta := -\ln[1 - \eta/(N_B + 1)]$.

Eqs. (14)-(15) comprise our first result. (15) shows that no QI system using signal energy \mathcal{N}_S can have an error probability exponent greater than $\beta\mathcal{N}_S$. In the low-background limit $N_B \simeq 0$, we have that $\beta \simeq \eta$ so the best possible exponent $\simeq \eta\mathcal{N}_S$. This matches that achieved by a classical transmitter (8) and is consistent with earlier no-go results for QI advantage in this regime [6, 28]. In the high-noise regime $N_B \gg 1$, the optimum exponent $\simeq \eta\mathcal{N}_S/N_B$ is attained by the TMSV QI system [3] (cf. (9)).

(14) explains why a TMSV QI system must use a large M in order to beat the classical performance (8) for any N_B . Intuitively, the right-hand side of (14) decreases the more the distribution $\{p_n\}$ is concentrated around its mean \mathcal{N}_S . The variance of the total signal photon number equals $\mathcal{N}_S(N_S + 1)$ for TMSV QI, and is minimized when the brightness $N_S \rightarrow 0$ for fixed \mathcal{N}_S . More precisely, evaluating (14) gives:

$$P_e^{\text{TMSV}} \geq \pi_0\pi_1 \left[1 + N_S \left(1 - \sqrt{1 - \eta/(N_B + 1)} \right) \right]^{-2M}. \quad (16)$$

Thus, for fixed M , the error probability of TMSV QI cannot decay exponentially with \mathcal{N}_S . However, if $M \rightarrow \infty$ for fixed \mathcal{N}_S , (16) allows the exponential scaling of (15).

B. Targets exhibiting flat Rayleigh fading

At optical wavelengths, most target surfaces are rough and our model of (1) involving deterministic and known values for η and ϕ needs modification. For such targets, one typically assumes a *Rayleigh fading* model [30, 31] when $h = 1$ in which η and ϕ are independent random variables with η distributed according to an exponential probability density $P(\eta)$ of mean $\bar{\eta}$ (the average reflectance of the target) and ϕ uniformly distributed over $[0, 2\pi]$. In addition, we will consider the *flat fading* limit in which the values of η and ϕ do not vary over the M signal modes. Such a model also describes optical propagation through the atmosphere [32] and was used in [11]. With these assumptions, ρ_1 in (5) is replaced by

$$\rho_1 = \frac{1}{2\pi} \int_0^1 d\eta \int_0^{2\pi} d\phi P(\eta) \left[\text{id}_I \otimes \left(\mathcal{U}_\phi \circ \mathcal{L}_{\eta, N_B^{(\eta)}} \right)^{\otimes M} \right] (\Psi) \quad (17)$$

while ρ_0 remains the same as before. In (17), $N_B^{(\eta)} = N_B/(1 - \eta)$ can vary greatly with η , but the model is a good approximation provided that $\bar{\eta} \ll 1$, as is the case in practice.

With some more work (see Appendix A for details), the approach of Sec. II A can be extended to give the lower bound

$$P_e^{\text{QI:fading}} \geq \pi_0\pi_1 / [1 + \bar{\eta}\mathcal{N}_S \ln(1 + 1/N_B)] \quad (18)$$

for any transmitter with signal energy \mathcal{N}_S . We see that for fading targets the error probability no longer decays exponentially with \mathcal{N}_S , generalizing the result of [11] derived for TMSV QI in the $N_S \ll 1, N_B \gg 1$ regime. In the same regime, it was shown that the sum frequency generation receiver of [10] can in principle achieve $P_e^{\text{TMSV}} \simeq \pi_1 / [1 + \bar{\eta}\mathcal{N}_S/N_B]$ for $\bar{\eta}\mathcal{N}_S/N_B \gg 1$, while the best classical transmitter has a P_e that is greater by a factor $\simeq \ln(\bar{\eta}\mathcal{N}_S/N_B)$ [11]. Comparing with (18), we see that the TMSV performance is essentially optimal over all transmitters with the same \mathcal{N}_S .

C. Estimation of target reflectance

Finally, we consider the problem of *estimating* the reflectance $\eta \ll 1$ of a detected specular target. The setup of Fig. 1 applies except that a target is known to be present and the joint quantum measurement of the returned signal and idler modes is aimed at generating an estimate $\check{\eta}$ of the target reflectance η . Instead of (5), we have a family of density operators $\{\rho_\eta\}$ given by

$$\rho_\eta = \left[\text{id}_I \otimes (\mathcal{U}_\phi \circ \mathcal{L}_{\eta, N_B^{(\eta)}})^{\otimes M} \right] (\Psi), \quad (19)$$

where, as before, Ψ is a general energy-constrained M -mode transmitter, $N_B^{(\eta)} = N_B/(1 - \eta)$, and ϕ is assumed to be known. The mean squared error $\text{MSE}_\eta = \mathbb{E}[(\check{\eta} - \eta)^2]$ of any unbiased estimator $\check{\eta}$ of η obeys the quantum Cramér-Rao bound [1, 25]:

$$\text{MSE}_\eta \geq \mathcal{K}_\eta^{-1} = \left[-4 \partial^2 F(\rho_\eta, \rho_{\eta'}) / \partial \eta'^2 \Big|_{\eta'=\eta} \right]^{-1}, \quad (20)$$

where \mathcal{K}_η is the *quantum Fisher information* (QFI) on η , and the equality relating QFI to fidelity is due to [33].

Using data processing arguments similar to those used for our target detection results, we can derive the upper bound

$$\mathcal{K}_\eta^{\text{QI}} \leq \mathcal{N}_S / [\eta(N_B + 1 - \eta)] \quad (21)$$

on the QFI valid for any Ψ , and the upper bound

$$\mathcal{K}_\eta^{\text{cl}} \leq \mathcal{N}_S / [\eta(2N_B + 1)] \quad (22)$$

on the QFI of any classical transmitter which is achieved using coherent states (see Appendix B for details). For $N_B = 0$, (21) recovers the result of [34] that is valid for all η and is achieved by a large class of transmitters. For $N_B > 0$ and $\eta \ll 1$, it is close to the upper bound on the QFI given in [9], but derived only for iid transmitters. In the presence of excess noise, (21) need not be saturable, but it was shown (see Eq. (6) of [9][35]) that the QFI of an M -mode TMSV transmitter is

$$\mathcal{K}_\eta^{\text{TMSV}} = [\mathcal{N}_S(1 + \mathcal{N}_S)] / [\eta(2\mathcal{N}_S N_B + \mathcal{N}_S + N_B + 1)]. \quad (23)$$

In the low-brightness limit $\mathcal{N}_S \rightarrow 0$, (23) approaches the bound (21) for all values of N_B when $\eta \ll 1$. Moreover, as argued in [9], this bound is achieved by the OPA receiver of [7]. From Eqs. (21)-(23), we see that the advantage of using quantum transmitters in the $\eta \ll 1$ regime is limited to at most a factor of 2 in the MSE.

III. DISCUSSION AND OUTLOOK

Our discussion of QI target detection falls within the Bayesian paradigm in which prior probabilities are assigned to the two hypotheses. Target detection is often described in the alternative Neyman-Pearson setting [25, 30] in which one asks for the best achievable detection probability $P_D = 1 - P_M$ for given P_F (which determines the so-called Receiver Operating Characteristic (ROC)). Various receivers for the TMSV transmitter have been studied in [12, 13, 19] in this paradigm, while [14] proved an asymptotic optimality result for TMSV QI. We note that the fidelity lower bounds developed here can be used to place upper bounds on the ROC curve of arbitrary QI transmitters (see, e.g., [36, 37]). We can also ask if adaptively chosen transmitter states can help in QI target detection – some suggestive results in this direction have appeared in [22, 38, 39].

Our reflectance estimation results show that the gain in using quantum transmitters is modest when $\eta \ll 1$. It is therefore interesting to explore quantum limits in detection and estimation in the region of moderate η and N_B , which is relevant to applications like quantum reading [40].

While further study of nonidealities in QI systems is necessary to assess their performance in real-world situations [19], our study delineates their ultimate capabilities for all ranges of system parameters.

FUNDING INFORMATION

This work was supported by the National Research Foundation and L'Agence Nationale de la Recherche Joint Project No. NRF2017-NRFANR004 VanQuTe, the National Research Foundation Singapore Fellowship No. NRF-NRFF2016-02, the Singapore Ministry of Education Tier 1 Grant RG190/17, and the FQXi Grant ‘Are quantum agents more energetically efficient at making predictions?’.

-
- [1] S. Pirandola, B. R. Bardhan, T. Gehring, C. Weedbrook, and S. Lloyd, “Advances in photonic quantum sensing,” *Nature Photonics* **12**, 724–733 (2018).
 - [2] Seth Lloyd, “Enhanced sensitivity of photodetection via quantum illumination,” *Science* **321**, 1463–1465 (2008).
 - [3] Si-Hui Tan, Baris I. Erkmen, Vittorio Giovannetti, Saikat Guha, Seth Lloyd, Lorenzo Maccone, Stefano Pirandola,

and Jeffrey H. Shapiro, “Quantum illumination with Gaussian states,” *Phys. Rev. Lett.* **101**, 253601 (2008).

- [4] BM Escher, RL de Matos Filho, and L Davidovich, “General framework for estimating the ultimate precision limit in noisy quantum-enhanced metrology,” *Nature Physics* **7**, 406–411 (2011).

- [5] Rafał Demkowicz-Dobrzański, Jan Kołodyński, and Mădălin Guță, “The elusive Heisenberg limit in quantum-enhanced metrology,” *Nature Communications* **3**, 1063 (2012).
- [6] Jeffrey H Shapiro and Seth Lloyd, “Quantum illumination versus coherent-state target detection,” *New Journal of Physics* **11**, 063045 (2009).
- [7] Saikat Guha and Baris I. Erkmen, “Gaussian-state quantum-illumination receivers for target detection,” *Phys. Rev. A* **80**, 052310 (2009).
- [8] Shabir Barzanjeh, Saikat Guha, Christian Weedbrook, David Vitali, Jeffrey H. Shapiro, and Stefano Pirandola, “Microwave quantum illumination,” *Phys. Rev. Lett.* **114**, 080503 (2015).
- [9] M. Sanz, U. Las Heras, J. J. García-Ripoll, E. Solano, and R. Di Candia, “Quantum estimation methods for quantum illumination,” *Phys. Rev. Lett.* **118**, 070803 (2017).
- [10] Quntao Zhuang, Zheshen Zhang, and Jeffrey H. Shapiro, “Optimum mixed-state discrimination for noisy entanglement-enhanced sensing,” *Phys. Rev. Lett.* **118**, 040801 (2017).
- [11] Quntao Zhuang, Zheshen Zhang, and Jeffrey H. Shapiro, “Quantum illumination for enhanced detection of Rayleigh-fading targets,” *Phys. Rev. A* **96**, 020302 (2017).
- [12] Quntao Zhuang, Zheshen Zhang, and Jeffrey H. Shapiro, “Entanglement-enhanced Neyman-Pearson target detection using quantum illumination,” *J. Opt. Soc. Am. B* **34**, 1567–1572 (2017).
- [13] Mark M. Wilde, Marco Tomamichel, Seth Lloyd, and Mario Berta, “Gaussian hypothesis testing and quantum illumination,” *Phys. Rev. Lett.* **119**, 120501 (2017).
- [14] Giacomo De Palma and Johannes Borregaard, “Minimum error probability of quantum illumination,” *Phys. Rev. A* **98**, 012101 (2018).
- [15] E. D. Lopaeva, I. Ruo Berchera, I. P. Degiovanni, S. Olivares, G. Brida, and M. Genovese, “Experimental realization of quantum illumination,” *Phys. Rev. Lett.* **110**, 153603 (2013).
- [16] Zheshen Zhang, Maria Tengner, Tian Zhong, Franco N. C. Wong, and Jeffrey H. Shapiro, “Entanglement’s benefit survives an entanglement-breaking channel,” *Phys. Rev. Lett.* **111**, 010501 (2013).
- [17] Zheshen Zhang, Sara Mouradian, Franco N. C. Wong, and Jeffrey H. Shapiro, “Entanglement-enhanced sensing in a lossy and noisy environment,” *Phys. Rev. Lett.* **114**, 110506 (2015).
- [18] S. Barzanjeh, S. Pirandola, D. Vitali, and J. M. Fink, “Microwave quantum illumination using a digital receiver,” arXiv e-prints , arXiv:1908.03058 (2019), arXiv:1908.03058 [quant-ph].
- [19] J. H. Shapiro, “The Quantum Illumination Story,” in *Proc. 2019 IEEE Int. Conf. on Microwaves, Antennas, Communications & Electronic Systems (COMCAS)* (2019) p. 1, see also arXiv:1910.12277 (2019).
- [20] Christian Weedbrook, Stefano Pirandola, Jayne Thompson, Vlatko Vedral, and Mile Gu, “How discord underlies the noise resilience of quantum illumination,” *New Journal of Physics* **18**, 043027 (2016).
- [21] Man-Hong Yung, Fei Meng, and Ming-Jing Zhao, “One-Shot Detection Limits of Quantum Illumination with Discrete Signals,” arXiv e-prints , arXiv:1801.07591 (2018), arXiv:1801.07591 [quant-ph].
- [22] Stefano Pirandola, Riccardo Laurenza, Cosmo Lupo, and Jason L Pereira, “Fundamental limits to quantum channel discrimination,” *npj Quantum Information* **5**, 1–8 (2019).
- [23] M. A. Nielsen and I. L. Chuang, *Quantum Computation and Quantum Information* (Cambridge University Press, 2000).
- [24] Alessio Serafini, *Quantum Continuous Variables: A Primer of Theoretical Methods* (CRC Press, 2017).
- [25] C. W. Helstrom, *Quantum Detection and Estimation Theory* (Academic Press, New York, 1976).
- [26] F Caruso, V Giovannetti, and A S Holevo, “One-mode bosonic Gaussian channels: a full weak-degradability classification,” *New Journal of Physics* **8**, 310 (2006).
- [27] Raúl García-Patrón, Carlos Navarrete-Benlloch, Seth Lloyd, Jeffrey H. Shapiro, and Nicolas J. Cerf, “Majorization theory approach to the Gaussian channel minimum entropy conjecture,” *Phys. Rev. Lett.* **108**, 110505 (2012).
- [28] Ranjith Nair, “Discriminating quantum-optical beam-splitter channels with number-diagonal signal states: Applications to quantum reading and target detection,” *Phys. Rev. A* **84**, 032312 (2011).
- [29] Koenraad M. R. Audenaert, “Comparisons between quantum state distinguishability measures,” *Quantum Information & Computation* **14**, 31–38 (2014).
- [30] H. L. Van Trees, *Detection, Estimation, and Modulation Theory: Part I*, 1st ed. (Wiley-Interscience, 2001).
- [31] Jeffrey H. Shapiro, “Target-reflectivity theory for coherent laser radars,” *Appl. Opt.* **21**, 3398–3407 (1982).
- [32] M. A. Khalighi and M. Uysal, “Survey on free space optical communication: A communication theory perspective,” *IEEE Communications Surveys Tutorials* **16**, 2231–2258 (2014).
- [33] Samuel L Braunstein and Carlton M Caves, “Statistical distance and the geometry of quantum states,” *Physical Review Letters* **72**, 3439 (1994).
- [34] Ranjith Nair, “Quantum-limited loss sensing: Multi-parameter estimation and Bures distance between loss channels,” *Phys. Rev. Lett.* **121**, 230801 (2018).
- [35] Ref. [9] reports the per-mode QFI $\mathcal{K}_{\sqrt{\eta}}/M$ on the reflectivity $\sqrt{\eta}$, which is related to \mathcal{K}_η via $\mathcal{K}_\eta = (\partial \sqrt{\eta} / \partial \eta)^2 \mathcal{K}_{\sqrt{\eta}}$.
- [36] Mankei Tsang and Ranjith Nair, “Fundamental quantum limits to waveform detection,” *Phys. Rev. A* **86**, 042115 (2012).
- [37] Mankei Tsang, “Quantum metrology with open dynamical systems,” *New Journal of Physics* **15**, 073005 (2013).
- [38] Tom Cooney, Milan Mosonyi, and Mark M. Wilde, “Strong converse exponents for a quantum channel discrimination problem and quantum-feedback-assisted communication,” *Communications in Mathematical Physics* **344**, 797–829 (2016).
- [39] Mario Berta, Christoph Hirche, Eneet Kaur, and Mark M. Wilde, “Amortized Channel Divergence for Asymptotic Quantum Channel Discrimination,” arXiv e-prints , arXiv:1808.01498 (2018), arXiv:1808.01498 [quant-ph].
- [40] Stefano Pirandola, “Quantum reading of a classical digital memory,” *Phys. Rev. Lett.* **106**, 090504 (2011).
- [41] Richard Jozsa, “Fidelity for mixed quantum states,” *Journal of Modern Optics* **41**, 2315–2323 (1994).

Appendix A: Targets exhibiting flat Rayleigh fading: Error probability lower bound for QI

We asserted in Sec. II B of the main text that, for targets exhibiting flat Rayleigh fading, the density operators of the joint return-idler system when the target is absent and present are given by

$$\rho_0 = \left[\text{id}_I \otimes \left(\mathcal{L}_{0,N_B}^{\otimes M} \right) \right] (\Psi), \quad (\text{A1})$$

$$\rho_1 = (1/2\pi) \int_0^1 d\eta \int_0^{2\pi} d\phi P(\eta) \left[\text{id}_I \otimes \left(\mathcal{U}_\phi \circ \mathcal{L}_{\eta, N_B^{(\eta)}} \right)^{\otimes M} \right] (\Psi) \quad (\text{A2})$$

respectively. It is usual in the classical radar literature to assume that $\sqrt{\eta}$ has a Rayleigh distribution – see, e.g., Sec. 4.4.2 of [30]. Then η itself has the exponential probability density $\tilde{P}(\eta) = (1/\bar{\eta}) \exp(-\eta/\bar{\eta})$ supported on $\eta \geq 0$. Strictly speaking, the probability that $\eta > 1$ should be zero since the target is a passive reflector. However, the above model is an excellent approximation classically as long as $\bar{\eta} \ll 1$, which is usually the case in practice.

Quantum mechanically, however, Eq. (1) of the main text does not represent a physically possible transformation if $\eta > 1$. To deal with this issue, we replace $\tilde{P}(\eta)$ with the truncated exponential density

$$P(\eta) = \begin{cases} \exp(-\eta/\bar{\eta}) / [\bar{\eta}(1 - e^{-1/\bar{\eta}})] & \text{if } \eta \in [0, 1] \\ 0 & \text{if } \eta \geq 1. \end{cases} \quad (\text{A3})$$

Again, if $\bar{\eta} \ll 1$, the discrepancy between (A3) and $P(\eta)$ is slight. It is the probability density (A3) that appears in (A2) and Eq. (17) of the main text.

We can now proceed to develop our error probability lower bound. First, we observe that the squared fidelity $F^2(\rho, \sigma)$, like $F(\rho, \sigma)$ itself [23], is concave in each of its arguments [41], so that we can write

$$F^2(\rho_0, \rho_1) \geq (1/2\pi) \int_0^1 d\eta \int_0^{2\pi} d\phi P(\eta) \\ \times F^2 \left\{ \rho_0, \left[id_I \otimes \left(\mathcal{U}_\phi \circ \mathcal{L}_{\eta, N_B^{(\eta)}} \right)^{\otimes M} \right] (\Psi) \right\}. \quad (A4)$$

Noting that the fidelity appearing in the integrand is ϕ -independent, we can apply the inequalities of Eqs. (12)-(13) of the main text to the fidelity and the bound $P_e[\sigma_0, \sigma_1] \geq \pi_0 \pi_1 F^2(\sigma_0, \sigma_1)$ used earlier to get the lower bound

$$P_e^{\Psi; \text{fading}} \geq \pi_0 \pi_1 \int_0^1 d\eta P(\eta) \left[\sum_{n=0}^{\infty} p_n \left(1 - \frac{\eta}{N_B + 1} \right)^{n/2} \right]^2 \quad (\text{A5})$$

on the average error probability of detecting a fading target. For any given transmitter Ψ with corresponding $\{p_n\}$, the right-hand side can be evaluated analytically in some cases, and numerically otherwise.

We can further derive an analytical transmitter-independent bound as follows. Applying Jensen's inequality to the quantity in brackets in (A5) gives

$$P_e^{\Psi; \text{fading}} \geq \pi_0 \pi_1 \int_0^1 d\eta P(\eta) \left(1 - \frac{\eta}{N_B + 1}\right)^{\mathcal{N}_S}. \quad (\text{A6})$$

For $N_B > 0$ and $0 \leq \eta \leq 1$, we have $1 - \eta/(N_B + 1) \geq \exp(-\gamma\eta)$, where $\gamma = \ln(1 + 1/N_B)$ is chosen such that the graph of $\exp(-\gamma\eta)$ intersects that of $1 - \eta/(N_B + 1)$ at $\eta = 0$ and $\eta = 1$. Substituting this lower bound into (A6) and evaluating the integral gives

$$P_e^{\text{QI; fading}} \geq \pi_0 \pi_1 \frac{1 - \exp(-\gamma \mathcal{N}_S - 1/\bar{\eta})}{[1 - \exp(-1/\bar{\eta})] (1 + \bar{\eta} \gamma \mathcal{N}_S)}, \quad (\text{A7})$$

$$\geq \frac{\pi_0 \pi_1}{1 + \bar{\eta} \gamma \mathcal{N}_S}, \quad (\text{A8})$$

which is Eq. (18) of the main text.

Appendix B: Estimation of target reflectance

As described in Sec. II C of the main text, for any transmitter Ψ , the density operator ρ_η of the returned signal and idler modes conditioned on the target reflectance having the value η is given by

$$\rho_\eta = \left[\text{id}_I \otimes \left(\mathcal{U}_\phi^{\otimes M} \circ \mathcal{L}_{\eta, N_B^{(\eta)}}^{\otimes M} \right) \right] (\Psi), \quad (\text{B1})$$

$$= \left[\text{id}_I \otimes \left(\mathcal{U}_\phi^{\otimes M} \circ \mathcal{A}_{N_B+1}^{\otimes M} \circ \mathcal{L}_{\eta/(N_B+1)}^{\otimes M} \right) \right] (\Psi), \quad (\text{B2})$$

where we have used the decomposition of Eq. (10) of the main text. Now note that the quantum channel $\mathcal{U}_\phi^{\otimes M} \circ \mathcal{A}_{N_B+1}^{\otimes M}$ that is applied ‘downstream’ to the S system is η -independent, and can be realized by coupling an ancilla mode A in a fixed state to the S system and evolving the joint system under a fixed unitary (this is the so-called Stinespring dilation of a quantum channel [23]). The monotonicity property of the QFI [42] then implies that the QFI on η achieved by making a measurement on the joint ISA system is at least as much as that on the IS system alone. On the other hand, the invariance of QFI under a known η -independent unitary transformation implies that the former value equals the QFI on η of the state family

$$\sigma_\eta = \left[\text{id}_I \otimes \mathcal{L}_{\eta/(N_B+1)}^{\otimes M} \right] (\Psi). \quad (\text{B3})$$

We have thus reduced the problem to maximizing the QFI on η for the outputs $\{\sigma_\eta\}$ of *pure-loss* channels under an energy constraint on the S modes. This problem was solved in [34] (cf. Eq. (14) therein), and transforming variables in that result gives the upper bound

$$\mathcal{K}_\eta^{\text{QI}} \leq \frac{\mathcal{N}_S}{\eta(N_B + 1 - \eta)} \quad (\text{B4})$$

for the QFI of any transmitter Ψ for any value of the excess noise N_B , which reproduces Eq. (21) of the main text.

Consider a single-mode coherent-state transmitter $|\psi\rangle_S = |\sqrt{\mathcal{N}_S}\rangle_S$ of energy \mathcal{N}_S . In order to evaluate the QFI on η , we first calculate the fidelity between the states ρ_η^{CS} and $\rho_{\eta'}^{\text{CS}}$ of (B1) for any two values η and η' . Using known results on the fidelity between Gaussian states (see e.g., Eq. (3.7) of [43]), we have

$$F(\rho_\eta^{\text{CS}}, \rho_{\eta'}^{\text{CS}}) = \exp \left[-\frac{(\sqrt{\eta'} - \sqrt{\eta})^2 \mathcal{N}_S}{4N_B + 2} \right] \quad (\text{B5})$$

The QFI then follows as

$$\begin{aligned} \mathcal{K}_\eta^{\text{CS}} &= -4 \frac{\partial^2 F(\rho_\eta^{\text{CS}}, \rho_{\eta'}^{\text{CS}})}{\partial \eta'^2} \Big|_{\eta'=\eta} \\ &= \frac{\mathcal{N}_S}{\eta(2N_B + 1)}. \end{aligned} \quad (\text{B6})$$

The additivity of the QFI for product states [42] and the linearity of the coherent-state QFI (B6) in the energy imply that (B6) is also the QFI of a multimode coherent state of total energy \mathcal{N}_S . Finally, any classical-state transmitter can be written as

$$\rho = \int_{\mathbb{C}^M} d^{2M} \alpha_I \int_{\mathbb{C}^M} d^{2M} \alpha_S, P(\alpha_I, \alpha_S) |\alpha_I\rangle \langle \alpha_I|_I \otimes |\alpha_S\rangle \langle \alpha_S|_S, \quad (\text{B7})$$

where $\alpha_S = (\alpha_S^{(1)}, \dots, \alpha_S^{(M)}) \in \mathbb{C}^M$ indexes M -mode coherent states $|\alpha_S\rangle_S$ of S , $\alpha_I = (\alpha_I^{(1)}, \dots, \alpha_I^{(M)}) \in \mathbb{C}^M$ indexes M -mode coherent states $|\alpha_I\rangle_S$ of I , and $P(\alpha_I, \alpha_S) \geq 0$ is a probability distribution. An average signal energy constraint of \mathcal{N}_S implies that $P(\alpha_I, \alpha_S)$ should satisfy

$$\int_{\mathbb{C}^M} d^{2M} \alpha_I \int_{\mathbb{C}^M} d^{2M} \alpha_S, P(\alpha_I, \alpha_S) \left(\sum_{m=0}^M |\alpha_S^{(m)}|^2 \right) = \mathcal{N}_S. \quad (\text{B8})$$

The convexity of the QFI [44], its invariance under adjoining an idler system in an η -independent state, and the linearity of the QFI (B6) in the energy then imply that the QFI of any classical probe satisfies

$$\mathcal{K}_\eta^{\text{cl}} \leq \frac{\mathcal{N}_S}{\eta(2N_B + 1)}, \quad (\text{B9})$$

which is Eq. (22) of the main text.